AFOSR-TR- 78-1280

PROGRESS REPORT NO. 1

LEVEL

THE KINETICS AND SPECTROSCOPY OF AIRCRAFT AND ROCKET PLUME CONSTITUENTS

By

Dr. F. P. Tully
Dr. A. R. Ravishankara
Co-Principal Investigators

DDC
RECEIVED
OCT 3 1978
F

June 1, 1977 - May 31, 1978

GEORGIA INSTITUTE OF TECHNOLOGY

Engineering Experiment Station
Atlanta, Georgia 30332

GTEES

1978

78 09 05 016

REPORT DOCUMENTATION PAGE		READ INSTRUCTIONS BEFORE COMPLETING FORM
1. REPORT NUMBER AFOSR-TR- 78 - 1 2 8 0	2. GOVT ACCESSION NO.	3. RECIPIENT'S CATALOG NUMBER
4. TITLE (and Subtitle) THE KINETICS AND SPECTROSCOPY OF AIRCRAFT AND ROCKET PLUME CONSTITUENTS		5. TYPE OF REPORT & PERIOD COVERED INTERIM
		6. PERFORMING ORG. REPORT NUMBER
7. AUTHOR(s) F. R. TULLY A. R. RAVISHANKARA		8. CONTRACT OR GRANT NUMBER(s) F49620-77-C-0111
9. PERFORMING ORGANIZATION NAME AND ADDRESS GEORGIA INSTITUTE OF TECHNOLOGY ENGINEERING EXPERIMENT STATION ATLANTA, GEORGIA 30332		10. PROGRAM ELEMENT, PROJECT, TASK AREA & WORK UNIT NUMBERS 2308B2 61102F
11. CONTROLLING OFFICE NAME AND ADDRESS AIR FORCE OFFICE OF SCIENTIFIC RESEARCH/NA BLDG 410 BOLLING AIR FORCE BASE, D C 20332		12. REPORT DATE 1978
		13. NUMBER OF PAGES 26
14. MONITORING AGENCY NAME & ADDRESS(if different from Controlling Office)		15. SECURITY CLASS. (of this report) UNCLASSIFIED
		15a. DECLASSIFICATION/DOWNGRADING SCHEDULE

16. DISTRIBUTION STATEMENT (of this Report)

Approved for public release; distribution unlimited.

17. DISTRIBUTION STATEMENT (of the abstract entered in Block 20, if different from Report)

18. SUPPLEMENTARY NOTES

19. KEY WORDS (Continue on reverse side if necessary and identify by block number)

RATE CONSTANTS	ARRHENIUS PLOTS	TIME RESOLVED UV ABSORPTION
HYDROCARBON OXIDATIONS	OXIDATION HALOBORANES	TIME RESOLVED IR SPECTROSCOPY
OH PLUS METHANE	FLASH PHOTOLYSIS	OXIDATION BY OZONE
OH PLUS HYDROGEN	RESONANCE FLUORESCENCE	
OH PLUS CARBON MONOXIDE	STOPPED FLOW MASS SPECTROMETRY	

20. ABSTRACT (Continue on reverse side if necessary and identify by block number)

Utilizing the technique of flash photolysis-resonance fluorescence the rate constants for the reactions of hydroxyl radicals (OH) with methane and carbon monoxide have been measured up to 825 K. Curvatures have been observed in the Arrhenius plots for both reactions. The measured rate constants have been compared with the previous measurements reported in the literature. Oxidation of BF_3 and BCl_3 by both O_2 and O_3 have been studied. The rate of oxidation of these haloboranes by O_2 is negligibly small. O_3 oxidizes BCl_3 (but not BF_3) at a measurable rate. These kinetics studies were carried out using time resolved

DD FORM 1473
1 JAN 73

UNCLASSIFIED

uv and I.R. absorption techniques as well as stopped flow mass spectrometry. Attempts have been made to understand the products and stoichiometry of the O_3 + BCl_3 reaction.

AIR FORCE OFFICE OF SCIENTIFIC RESEARCH
CONTRACT NO. F 49620-77-C-0111
PROGRESS REPORT NO. 1

THE KINETICS AND SPECTROSCOPY OF
AIRCRAFT AND ROCKET PLUME CONSTITUENTS

June 1, 1977 - May 31, 1978

By

Energy and Environmental Analysis Division
Applied Sciences Laboratory
Engineering Experiment Station
Georgia Institute of Technology
Atlanta, Georgia   30332

Co-Principal Investigators:
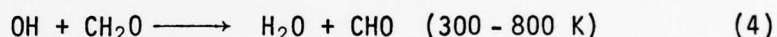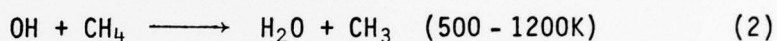
Dr. F.P. Tully   Dr. A.R. Ravishankara

July 31, 1978

Chemical kinetic studies of relevance to aircraft and rocket exhaust plume characterization are in progress. These investigations are divided between two topic areas: (1) hydroxyl radical - small molecule rate constant measurements, and (2) kinetic and mechanistic probes of oxidant - haloborane reactions. These topic areas are described individually below.

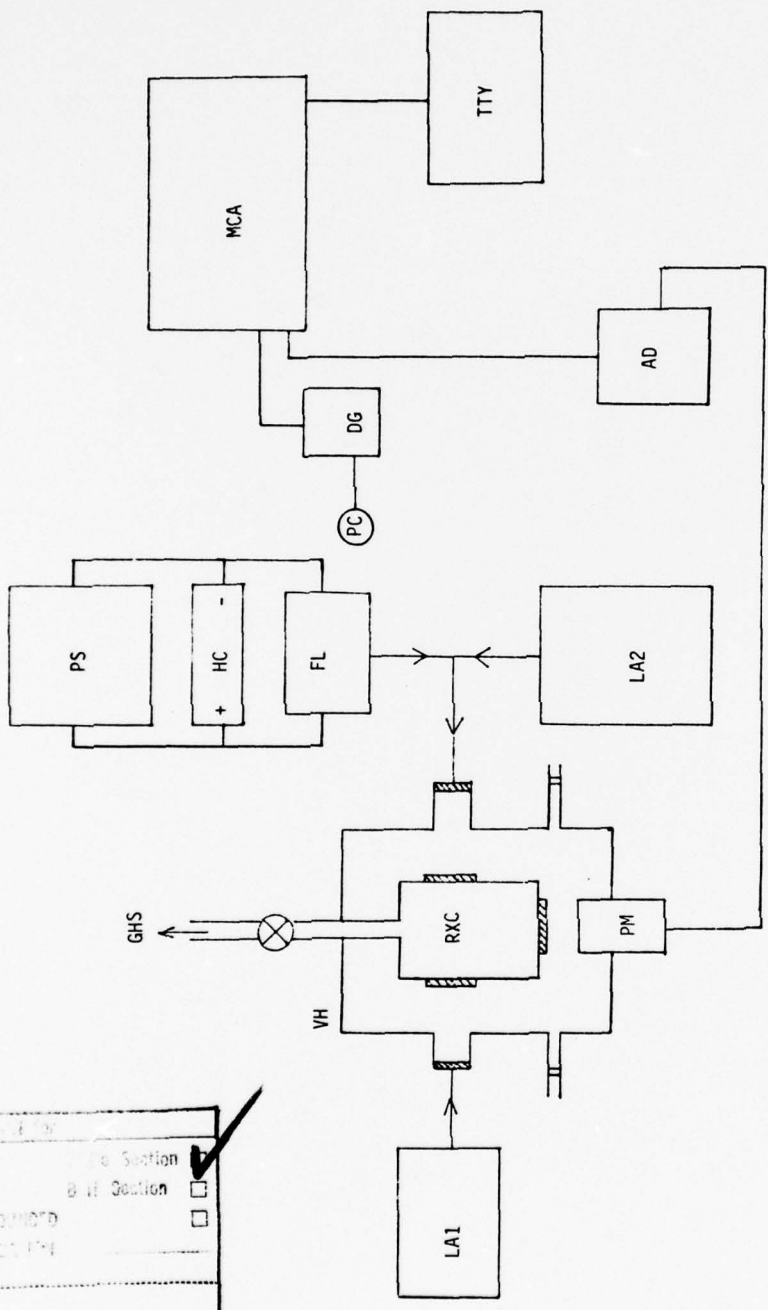## I. Hydroxyl Radical - Small Molecule Rate Constant Measurements

Using the technique of flash photolysis - (resonance/laser induced) fluorescence, we are measuring absolute rate constants for Reactions (1) - (4) over the indicated temperature intervals.

$$OH + H_2 \longrightarrow H_2O + H \quad (500 - 1200K) \qquad (1)$$

$$OH + CH_4 \longrightarrow H_2O + CH_3 \quad (500 - 1200K) \qquad (2)$$

$$OH + CO \longrightarrow H + CO_2 \quad (500 - 1000K) \qquad (3)$$

$$OH + CH_2O \longrightarrow H_2O + CHO \quad (300 - 800 \text{ K}) \qquad (4)$$

In these experiments, a spark discharge through an inert gas produces a radiation flash composed of wavelengths from the vacuum ultraviolet through the visible spectral regions. The radiation flash is transmitted to the reaction cell in which H_2O is photolyzed to produce H and OH species. The post-flash temporal behavior of the OH concentration is then monitored via resonance/laser-induced fluorescence.

A block diagram of the overall reaction kinetics system is shown in Figure 1. The basic components of this system are: (1) a thermostated reaction cell centered in a vacuum housing, (2) a spark discharge flashlamp perpendicular to one face of the cell, (3) a resonance lamp (or probe laser) perpendicular to another face of the cell, (4) a photodetector perpendicular

1

AD - Amplifier discriminator
FL - Flash lamp
HC - High voltage capacitor
LA1 - Argon ion laser/resonance
      lamp

LA2 - Laser for production of
      free radicals
MCA - Multi-channel analyzer
PC - Photocell

PM - Photomultiplier
PS - Power supply
RXC - Reaction cell
TTY - Teletype
VH - Vacuum housing

Figure 1. Reaction Kinetics System

to the base of the cell, and (5) fast photon counting electronics, including a multichannel analyzer which provides up to 1 μsec time resolution and signal averaging capabilities.

To this point in time, all of the data on Reactions (1)-(4) which we have collected has been obtained using resonance lamp excitation of OH fluorescence. We have found, not surprisingly, that as the reaction temperature is raised the OH radical detection sensitivity decreases markedly. Factors such as increasing nonradiative collisional deactivation of the $A^2\Sigma^+$ state of OH, decreasing usable H_2O number densities and decreasing optical transmission to and from the reaction zone contribute to this diminution of detection sensitivity at higher temperatures. Sensitivity limitations have necessitated several modifications of our initial experimental configuration: (1) improved quartz lens focussing of the resonance radiation; (2) teflon blackening of the inside of the vacuum housing so as to minimize scattered resonance radiation; (3) improved collimation and cooling throughout the system; and (4) installation of counting electronics linear up to pulse rates of 20 MHz. As we approach 1000K experiments, further improvements are in the works. We plan to install a quartz light pipe between the resonance lamp and the quartz focussing lens attached to the reaction cell. We also plan to add a quartz focussing lens at the base of the reaction cell to improve the photomultiplier collection efficiency. Two possible further changes are also receiving consideration: (1) replacement[1] of the flowing inert gas spark discharge flashlamp by a closed xenon flashlamp, and (2) purchase and installation of a new Varian photomultiplier tube having nearly twice the quantum efficiency at 3100Å of our present RCA 8850 photodetector.

Two other approaches to this detection sensitivity problem are also

3

receiving attention. During this contract period, a 4-watt Lexel argon ion laser and an assortment of mirror mounts and optical components were purchased using State of Georgia funds. Intracavity doubled and extracavity doubled cw ultraviolet dye laser systems were built and tuned to an OH fluorescence excitation wavelength at 3082.5Å. Use of such a cw laser probe to excite OH fluorescence would be extremely advantageous since the scattered light background so characteristic with resonance lamp excitation could be almost totally negated. At present, however, due to low power densities and a high-loss doubling crystal, insufficient usable photon flux has been obtained. Future modifications of this laser probe must therefore involve construction of an intracavity doubled ring dye laser system. Progress toward this end will depend on the availability of in-house funds.

An alternative laser-based approach involves the use of our high-power pulsed Quantel YG-481A Nd/Yag laser. Since harmonic generation efficiencies are proportional to power densities, frequency doubling of pulsed tunable dye laser radiation would certainly provide sufficient radiant flux to excite the needed OH fluorescence levels. Unfortunately, such a transition from a cw detection system to a pulsed detection system greatly hinders the obtainable duty cycle of the kinetic measurements. One would have to trigger the firing of the exciting laser probe at various fixed times following the initiating photolysis flash in order to generate a concentration vs. time profile. Normalization constraints would thus also become much more severe. Realization of this detection system, then, though tremendously promising, is still quite some time off.

During this contract year, then, our efforts within this topic area have been interactively time-shared between data acquisition and detection technology improvement. Using our present resonance lamp excitation

4

detection mode, quality rate constant measurements are accessible to temperatures of 1000K. In the following paragraphs, preliminary rate constant data for Reactions (2) and (3) up to temperatures in excess of 800K will be discussed. Following the presentation of these results, the status of our studies of Reactions (1) and (4) will be discussed.

Figure 2a presents a typical example of our measured OH concentration vs. time profiles (following scattered light background subtraction) in the absence and presence of molecular reactant. In the pseudo-first order kinetic approximation, the measured pseudo-first order decay constant, k_{exp}, is given by the expression

$$k_{exp} = k_{bi}[\text{Reactant}] + k' \quad ,$$

where k_{bi} is the bimolecular rate constant for the reaction OH + Reactant → Products and k' represents the rate of loss of OH from the viewing zone of the photomultiplier in the absence of the subject reactant. The value of k_{bi} is then determined from the slope of a plot of k_{exp} vs. [Reactant]. For the OH + CO → H + CO_2 reaction at 511K, such a plot, typical for our measurements, is displayed in Figure 2b.

Absolute rate constant vs. temperature data for Reaction (2) is listed in Table I and plotted in Arrhenius form in Figure 3. Analogous measurements for Reaction (3) are listed in Table II and plotted in Arrhenius form in Figure 4. The precision for all of these measurements is 15% or better. These numbers should nevertheless be considered preliminary for two reasons: (1) for the most part least squares analyses of the OH decay rates and the k_{exp} vs. [Reactant] plots have not yet been performed, and (2) at a limited number of temperatures, measurements at one or two

5

OH + CO $\longrightarrow$ H + CO$_2$ (511 K)
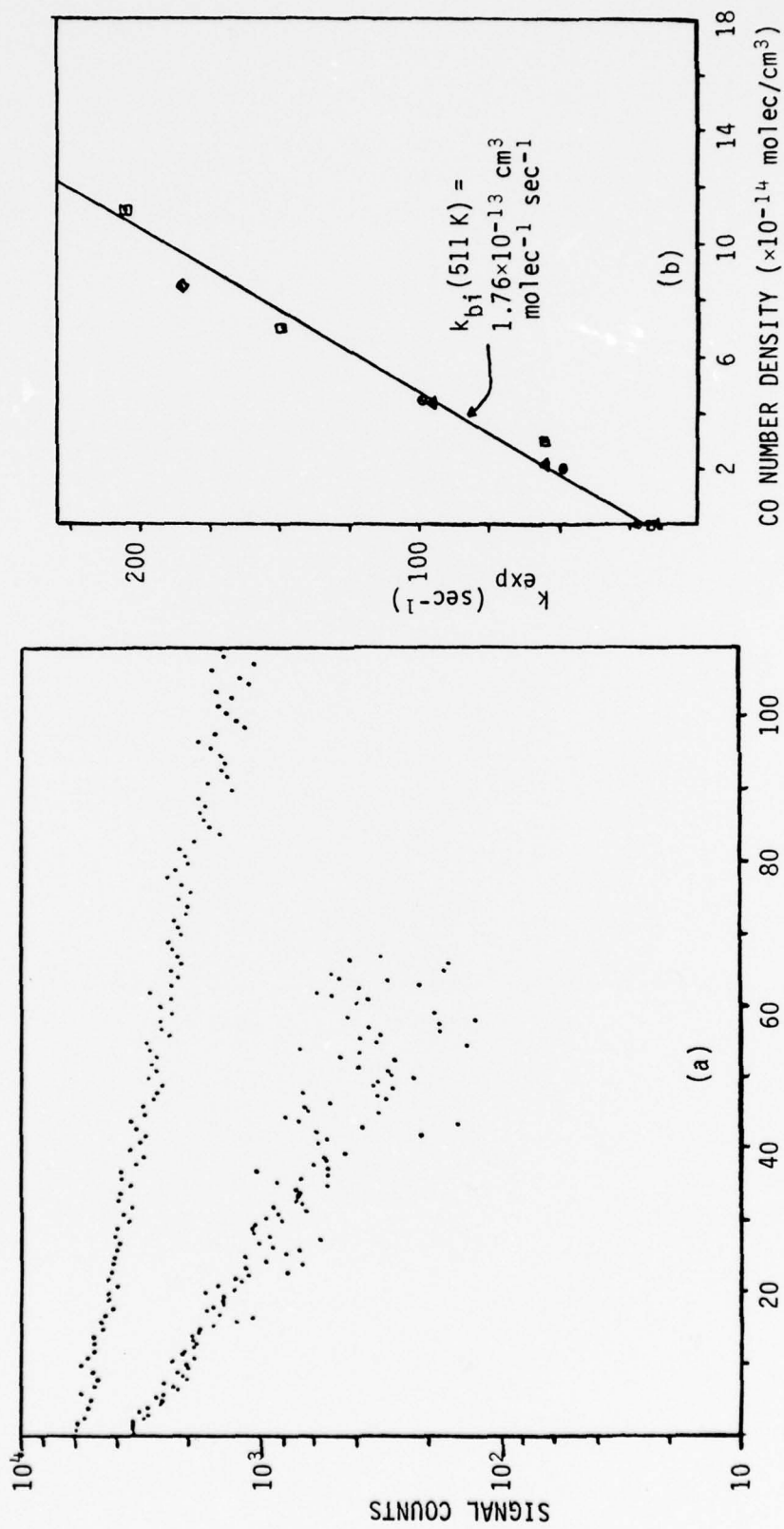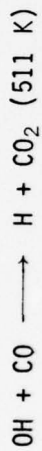
--Upper curve: OH decay in the absence of CO;
Lower curve: OH decay at a CO partial pressure of 0.0107 Torr.

Figure 2

6

Table I. Bimolecular Rate Constant vs. Temperature for Reaction (2)

$$OH + CH_4 \rightarrow CH_3 + H_2O$$
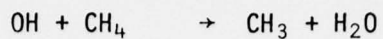
Temperature (K)	Bimolecular Rate Constant K_{bi} (cm^3 molec^{-1} sec^{-1})
298	7.45×10^{-15}
374	2.35×10^{-14}
398	4.59×10^{-14}
453	9.03×10^{-14}
511	1.62×10^{-13}
600	3.10×10^{-13}
718	7.36×10^{-13}
825	1.07×10^{-12}
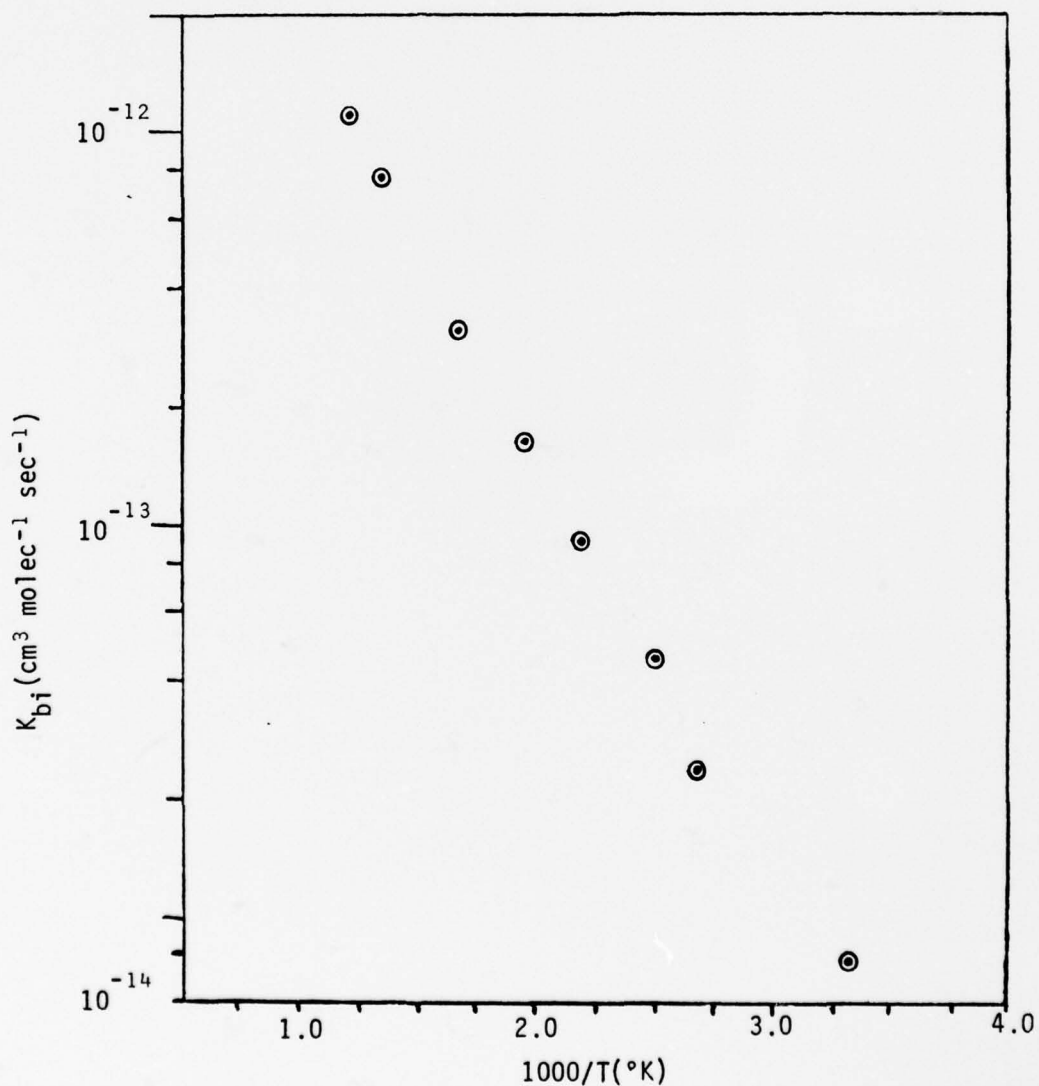
Figure 3

Table II. Bimolecular Rate Constant vs. Temperature for Reaction (3)

$$OH + CO \longrightarrow CO_2 + H$$
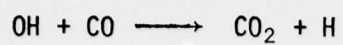
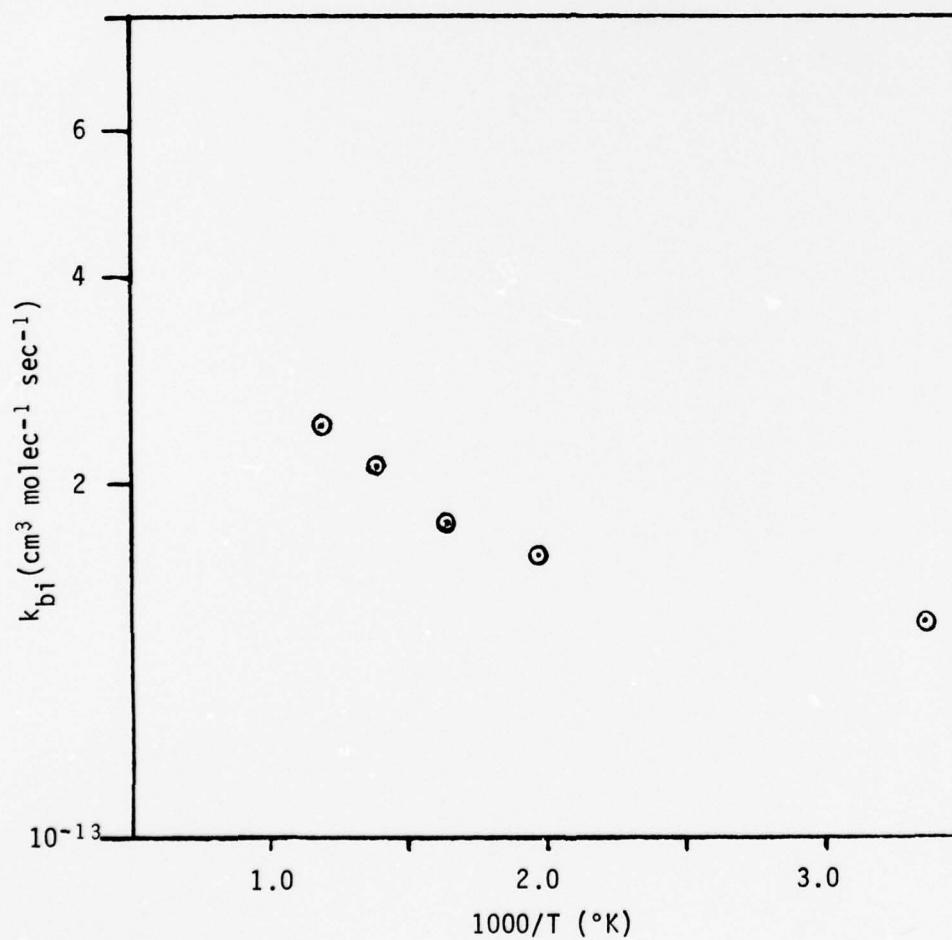| Temperature (K)	Bimolecular Rate Constant K_{bi} (cm^3 molec^{-1} sec^{-1})
298	1.53×10^{-13}
511	1.76×10^{-13}
610	1.88×10^{-13}
718	2.12×10^{-13}
833	2.31×10^{-13}

Figure 4

8

more reactant concentrations are desired.

Our results for Reaction (2), $OH + CH_4 \rightarrow H_2O + CH_3$, are in qualitative agreement with the flash photolysis - resonance absorption measurements of Zellner and Steinert.[2] Curvature in the Arrhenius plot is observed, though the degree of such curvature appears substantially less severe than that reported in Reference 2. A closer examination of this comparison will be presented in future reports.

Our rate constant measurements for Reaction (3), $OH + CO \rightarrow H + CO_2$, are in very close agreement with those calculated from the analytical expression recommended in the recent review of Baulch et al.[3] The low-temperature regime activation energy for this reaction is indeed very small.

Although a substantial number of experiments have been performed on the kinetics of Reaction (1), $OH + H_2 \rightarrow H_2O + H$, we have not included those results in this report. The precision of these rate constant measurements has not been as good as that obtained in the studies of Reactions (2) and (3). We feel that a number of these experiments require thorough reinvestigation prior to the dissemination of these results.

Kinetic studies of Reaction (4), $OH + CH_2O \rightarrow H_2O + CHO$, are just beginning in earnest. For these experiments it has proven to be necessary to synthesize monomeric formaldehyde from paraformaldehyde. Because water is known to catalyze the polymerization of formaldehyde, only small quantities of this photolytic source can be tolerated. [At low temperatures, OH will be formed in the presence of CH_2O by 2650Å laser photolysis of an $O_3/H_2/CH_2O$ mixture.] We expect, then, to have to live with very small signals (and much averaging) in the higher temperature regime of this experiment where H_2O is used as the photolytic source of OH.

9

In the next few months we expect to extend the temperature intervals of measurement for these reactions and, in particular, address the study of Reactions (1) and (4) in much more detail. An analogous study of the $OH + C_2H_6 \rightarrow H_2O + C_2H_5$ reaction is planned during the second year of the contract.

II. Oxidant - Haloborane Studies

The achievement of an understanding of the oxidation characteristics of halogenated boron species is essential to the estimation of the concentrations of boron molecular emitters present in advanced fuel rocket plume exhausts. Knowledge of the typical concentrations of emitting species is a prerequisite to the interpretation of rocket plume infrared signatures. Since very little is known about haloborane oxidation (and also about the technology required for its study), we have initiated studies of relevant molecular reactions with the aim of developing experimental techniques permitting future investigation of the more complex radical reactive systems.

In the work statement for this program, we have contracted to measure absolute rate constants for Reactions (5) and (6),

$$O_2 + BF_3 \longrightarrow \text{Products} \tag{5}$$

$$O_2 + BCl_3 \longrightarrow \text{Products,} \tag{6}$$
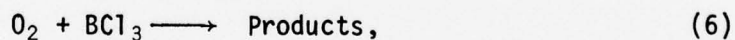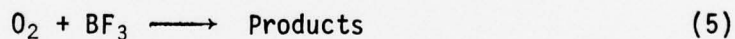
using the technique of stop-flow time-of-flight mass spectrometry. A schematic diagram of this technique is displayed in Figure 5. In this system a thermostated reaction vessel equipped with a very small molecular leak is positioned directly above the ion source of a time-of-flight mass spectrometer. Reactants are admitted to the vessel and mix homogeneously

10

AM – amplifier
AS – analog scanner
DP – diffusion pump
EB – electron beam
MEM – magnetic electron multiplier
OS – oscilloscope
RC – reaction chamber
SB – sample bulb
SV – solenoid valve
TB – temperature bath-circulating pump
TJ – temperature jacket
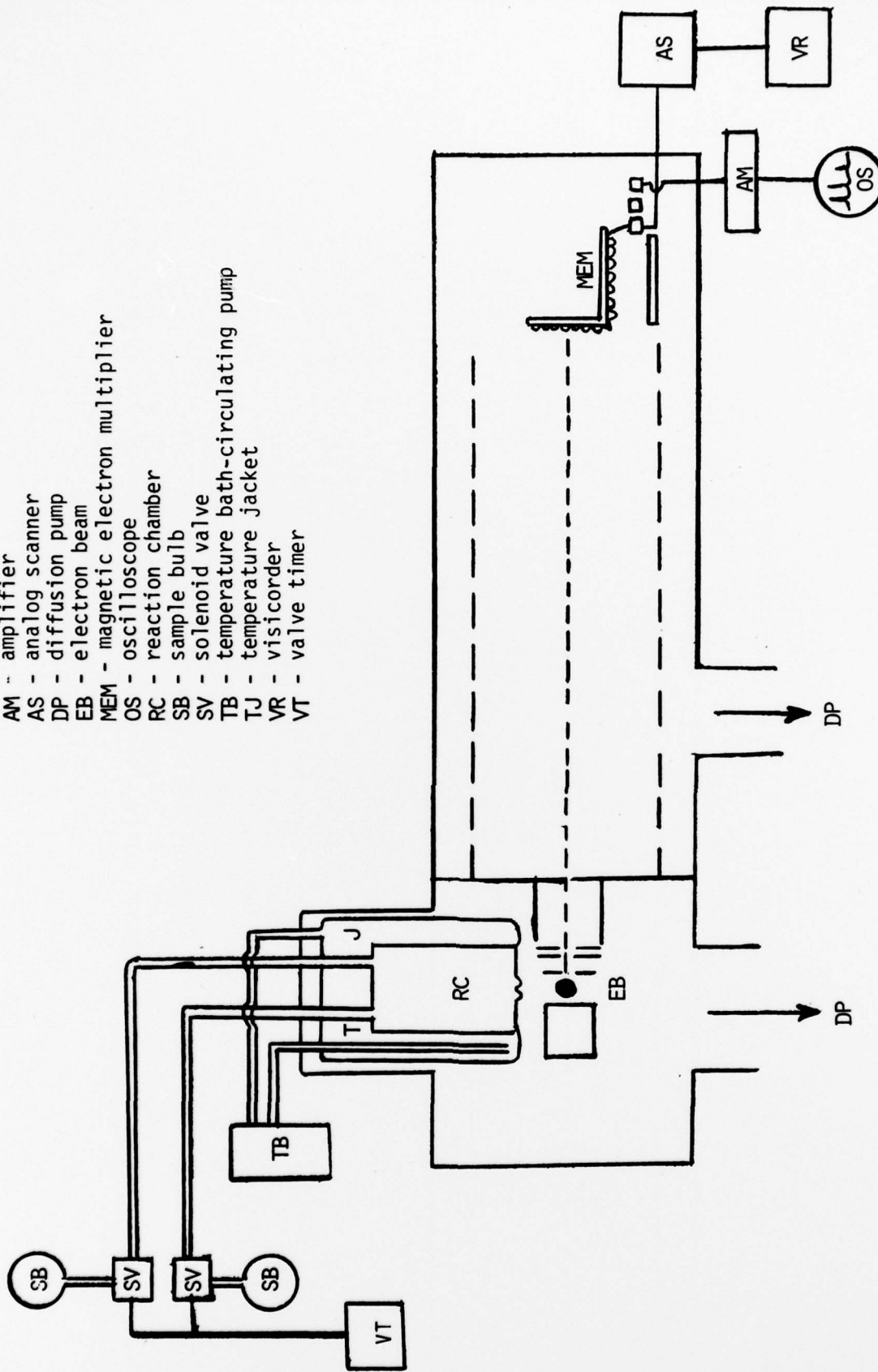VR – visicorder
VT – valve timer

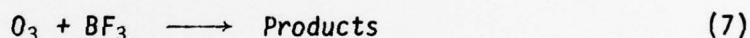FIGURE 5 – STOP-FLOW TOF MASS SPECTROMETER SYSTEM

11

and reach temperature equilibrium within a few milliseconds. Following
mixing, the reaction is occurring at the desired conditions of tempera-
ture, pressure and reactor composition. The molecular leak at the bottom
of the reaction cell allows a very small fraction of the cell contents to
diffuse into the ion source of the mass spectrometer. This effluent is
ionized, the ions are accelerated to constant energy, and the ion current
and time of arrival at the detector are measured. The entire spectrum
can be cycled every 100 μsec. In essence, this technique allows the de-
termination of the cell contents in real time. In a kinetic experiment,
however, only one ion, produced upon ionization of either a reactant or
product molecule, is monitored with time. The temperature range of our
stop-flow system is 250K - 450K. Second order reaction rate constants
between 2×10^{-23} cm^3 molec^{-1} sec^{-1} and 5×10^{-17} cm^3 molec^{-1} sec^{-1} are amen-
able to accurate measurement within this system. Since this range of
rate coefficients corresponds to that expected for many molecule-molecule
reactions, this technique was proposed for the study of Reactions (5) and
(6).

When stop-flow time-of-flight mass spectrometry experiments were
performed on Reactions (5) and (6), it was found that within experimental
error addition of one reactant to the reaction vessel had no effect on
the rate of disappearance of the other reactant. We thus estimated that
the rate constants for these processes are $\leq 1\times10^{-23}$ cm^3 molec^{-1} sec^{-1}.

Having found that the rate constants for Reactions (5) and (6) are
too slow to be measured by the above technique, we devised a time-resolved
infrared spectroscopy study of these reactions. An optical absorption
cell seasoned with the haloborane prior to each experiment was filled with
a few torr of the haloborane and 350 - 500 torr of oxygen. Haloborane in-

12

frared absorption intensities were then monitored as functions of time.
Typical results of these experiments are plotted in Figure 6. The halo-
borane decay rates are seen to be extremely slow and, because wall loss
effects may have been contributing to the observed decays, the rate con-
stants extracted from these pseudo-first order decays must be considered
as upper limits. Our knowledge of these rate constants thus remains
limited to the expressions $k_5 \leq 1 \times 10^{-30}$ cm^3 molec^{-1} sec^{-1} and $k_6 \leq 4 \times 10^{-25}$
cm^3 molec^{-1} sec^{-1}.

Having observed nearly negligible reactivities for the reactions
$O_2 + BF_3/BCl_3$, we decided to probe the general oxidative behavior of the
haloboranes in more detail by studying their reactions with more active
oxidizing agents. Investigations of the following reaction processes were
made:

$$O_3 + BF_3 \longrightarrow \text{Products} \tag{7}$$

$$O_3 + BCl_3 \longrightarrow \text{Products} \tag{8}$$

$$H_2O + BCl_3 \longrightarrow \text{Products} . \tag{9}$$

Again using the technique of time-resolved infrared spectroscopy, Reaction
(7) was investigated and found to be immeasurably slow at room temperature.
This reaction, then, was not looked at further. The study of Reaction (8),
on the other hand, proved to be very interesting. Time-sequenced sets of
complete infrared spectra of reacting $O_3/BCl_3/Ar$ mixtures were taken. The
initial BCl_3 and argon pressures were measured using a capacitance manom-
eter and the initial O_3 pressure was calculated from uv absorption measure-
ments made at 313 nm. The initial reactant partial pressures were varied
by as much as factors of four in different runs. The BCl_3 and O_3 decay

13

$$O_2 + BCl_3 \longrightarrow \text{Products}$$

$$P^0_{BCl_3} = 1.1 \text{ Torr}; \quad P^0_{O_2} = 380 \text{ Torr}$$

$$\text{SLOPE} = k' = 4.89 \times 10^{-6} \text{ sec}^{-1}$$

$$k_{bi} \leq 4 \times 10^{-25} \text{ cm}^3/\text{molec} \cdot \text{sec}$$

TIME AFTER MIXING
(Minutes)

$$O_2 + BF_3 \longrightarrow \text{Products}$$

$$P^0_{BF_3} = 2.3 \text{ Torr}; \quad P^0_{O_2} = 460 \text{ Torr}$$
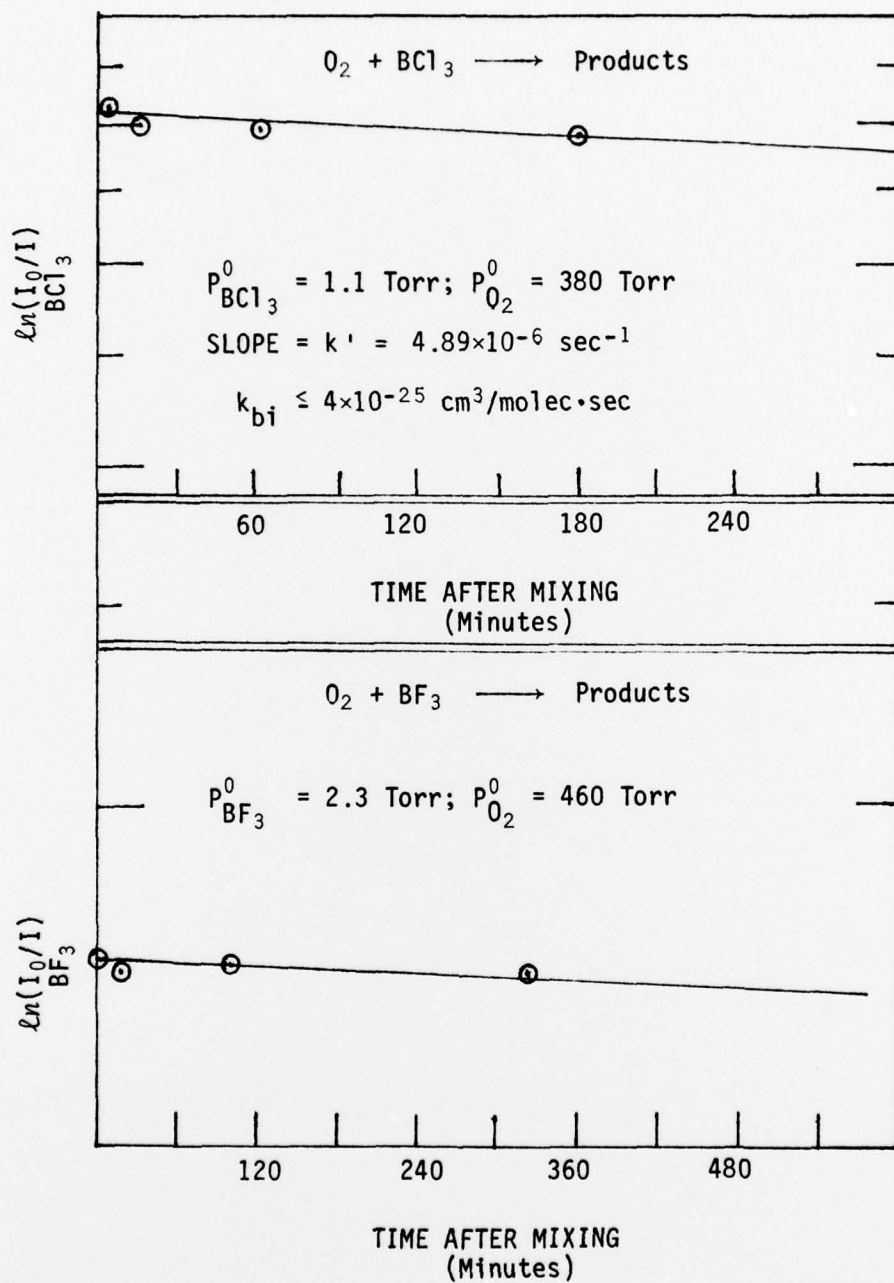
TIME AFTER MIXING
(Minutes)

Figure 6. Time-Resolved Infrared Spectroscopy

14

rates and reaction product buildup rate (as shown in Figure 7a, a reaction product peak not observed in the pure O_3 or pure BCl_3 spectra grows with time) are calculated from the peak intensities in the sequential infrared spectra. Relative concentration vs. time after mixing plots for a typical experimental run are displayed in Figure 7b. It is seen that the rate of growth of the reaction product closely images the rate of decay of the BCl_3 reactant. It is worth noting here, however, that the bimolecular rate constants calculated from such plots do show a slight tendency to increase with increasing $[O_3]_{t=0}/[BCl_3]_{t=0}$ ratios. These variations are likely due to the overall stoichiometry of the reaction.

Three other experimental techniques were applied to the study of Reaction (8): (1) time-resolved uv absorption spectroscopy, (2) stop-flow time-of-flight mass spectrometry, and (3) reaction end product analysis. The results of these studies will be discussed below in turn.

A schematic diagram of the simple but very powerful technique of time-resolved uv absorption spectroscopy is given in Figure 8a. Light from a mercury lamp at 2537Å was passed through an absorption cell containing the $O_3/BCl_3/Ar$ mixture. The transmitted intensity was monitored as a function of time by a filtered photodiode. Experiments were run with $[BCl_3]$ in varying excesses over $[O_3]$, ozone being the monitored species. Use of this technique required considerable caution. Since 2537Å radiation is absorbed by ozone via the photodissociative reaction $O_3 \xrightarrow{h\nu} O(^1D) + O_2$, the possibility existed that the atomic oxygen formed in the probe process could contribute to the chemistry under study. By using a variety of ozone concentrations and 2537Å radiation fluxes, however, it was conclusively shown that such probe-induced processes were unimportant. Furthermore, by allowing the low concentration reactant ozone to undergo complete

15

$O_3 + BCl_3 \longrightarrow$ PRODUCTS

WAVELENGTH (MICRONS)

$t = 0$; $P^0_{BCl_3} = 0.59$ Torr; $P^0_{O_3} = 4.03$ Torr

$t = 60$ minutes

% TRANSMISSION

RXN PRODUCT

O_3 O_3

BCl_3

BCl_3

RXN PRODUCT

O_3 O_3

BCl_3

BCl_3

WAVENUMBER (CM^{-1})
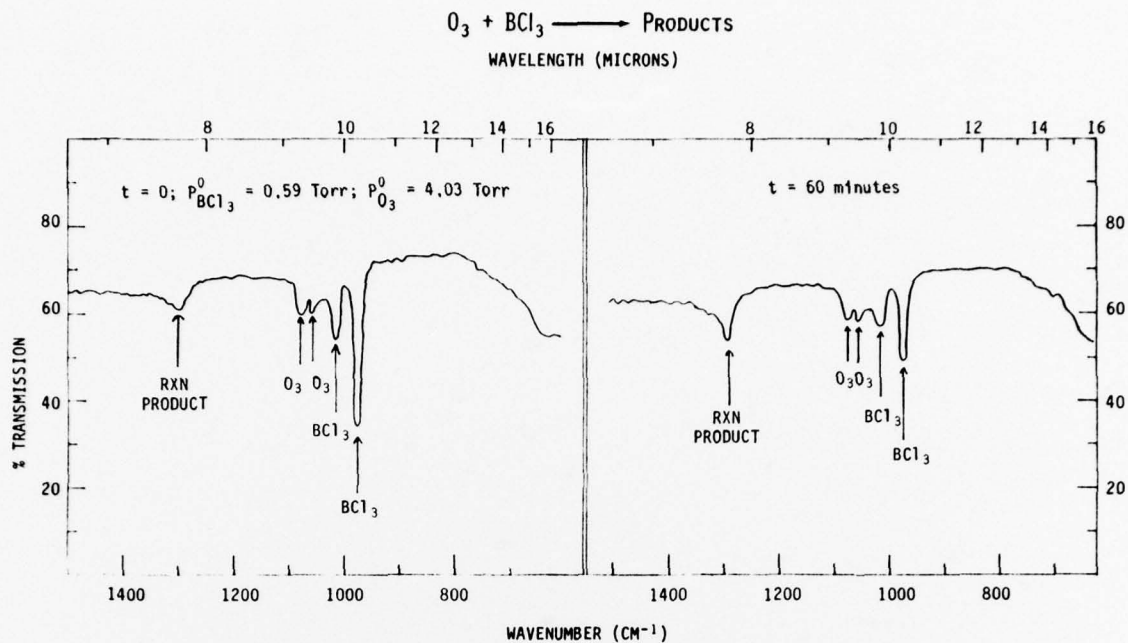
Figure 7a.   Time-Resolved Infrared Spectroscopy

at $t=0$, $P^0_{BCl_3} = 0.59$ Torr, $P^0_{O_3} = 4.03$ Torr

$Ln(I_0/I)$ BCl$_3$

$k' = 2.1 \times 10^{-4}$ sec^{-1}

$Ln(I_0/I)$ O$_3$

[O$_3$] decreased by ~10% during course of expt.

Figure 7b.

$Ln(\Delta I_{t=\infty} - \Delta I_{t=t})$ PRODUCT

$k' = 2.0 \times 10^{-4}$ sec^{-1}

$k_{b1} = 1.61 \times 10^{-21}$ cm^3/molec sec

TIME AFTER MIXING
(Minutes)

GHS

Hg lamp   Quartz Cell   **2537** Filter   Photo Diode   HV

Electrometer
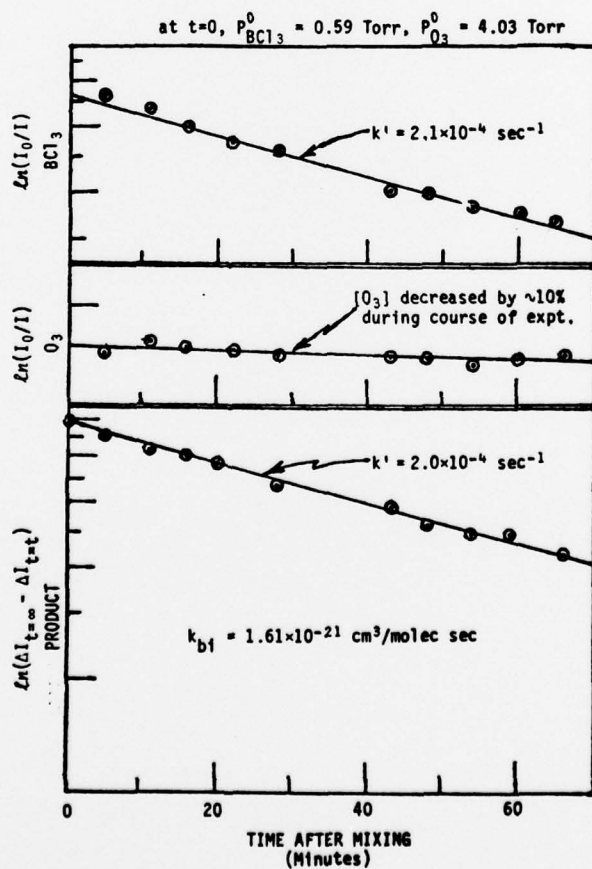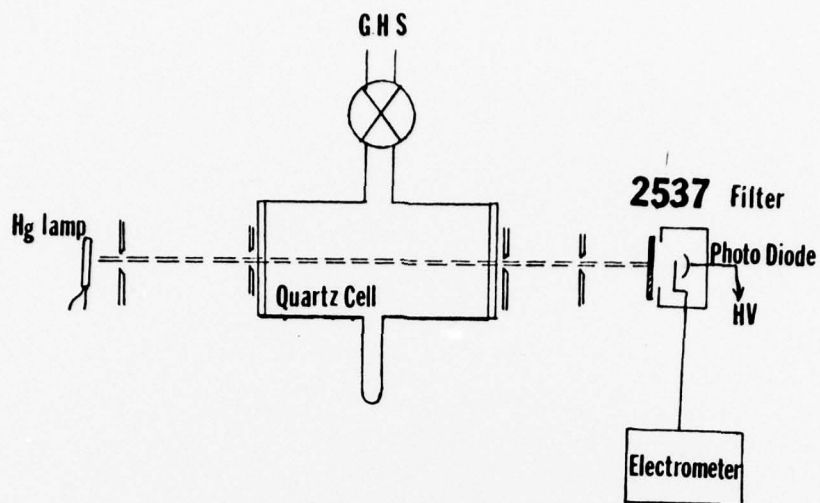
TIME RESOLVED UV ABSORPTION

Figure 8a

$O_3 + BCl_3 \longrightarrow$ PRODUCTS

⊙ $[O_3]_{t=0}$ = 2-3×10^{15} molec/cm^3; lamp flux "high"
△ $[O_3]_{t=0}$ = 3×10^{15} molec/cm^3; lamp flux "low"
⊡ $[O_3]_{t=0}$ = 8.5×10^{14} molec/cm^3; lamp flux "low"

SLOPE = 2.66×10^{-4} sec^{-1} torr^{-1}
k_{bi} = 8.31×10^{-21} cm^3/molec·sec

K' (10^{-3} SEC^{-1})

BCl$_3$ PRESSURE (TORR)
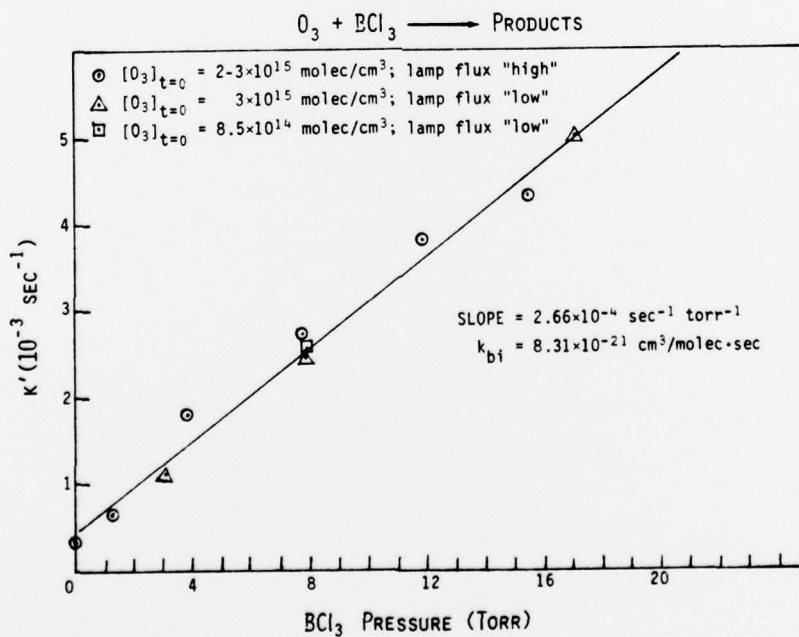
Figure 8b

17

reaction and then measuring essentially no absorption of 2537Å radiation, it was clearly demonstrated that the products of the reaction were not absorbing the probe radiation and thereby biasing the kinetic results. Thus the time variation of the transmitted 2537Å intensity generates an accurate time history of the ozone concentration. The experiments were run under pseudo-first order conditions with BCl_3 in excess and, as shown in Figure 8b, the bimolecular rate constant was obtained as the slope of a plot of the pseudo-first order decay constant vs. the BCl_3 concentration. A value of k_{bi} (298K) = 8.31×10^{-21} cm^3 $molec^{-1}$ sec^{-1} was obtained.

Reaction (8) was also studied by the previously described technique of stop-flow time-of-flight mass spectrometry. Small concentrations of BCl_3 in varying excesses of ozone were mixed in the reaction vessel and the time variation of the BCl_2^+ ion was followed mass spectrometrically. Typical decay curves are shown in Figure 9a; a bimolecular rate constant of k_{bi} = 1.2×10^{-20} cm^3 $molec^{-1}$ sec^{-1} was calculated by the usual methods. Averaging this result with that obtained using time-resolved uv absorption spectroscopy techniques, one obtains a room temperature rate constant for Reaction (8) of k_{bi} = $(1.0 \pm 0.3) \times 10^{-20}$ cm^3 $molec^{-1}$ sec^{-1}. It is worth noting here that this value exceeds that obtained in the time-resolved infrared spectroscopy experiments (see Figure 7) by about a factor of six. Though we do not feel that we can adequately explain this discrepancy, it is probable that it is at least in part related to wall absorption of ozone in the extended duration infrared spectroscopy experiments.

Mass spectrometric studies of Reaction (8) were also performed by time sequenced sweeps of the entire mass spectrum. From top to bottom, Figure 9b shows respectively the mass spectrum obtained for pure ozone, that obtained for pure BCl_3, and that obtained a substantial period of

18

O$_3$

BCl$_3$

O$_3$ + BCl$_3$ ⟶ Products

O$_3$ in large excess

MASS NUMBER
(A.M.U.)

Figure 9b

[O$_3$]0 torr

[O$_3$]1.5 torr

[O$_3$]4 torr

k·1.2×10^{-20} cc·molec.$^{-1}$ sec^{-1}
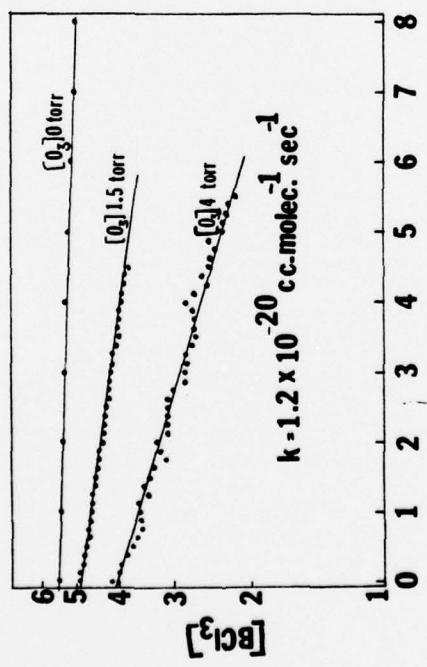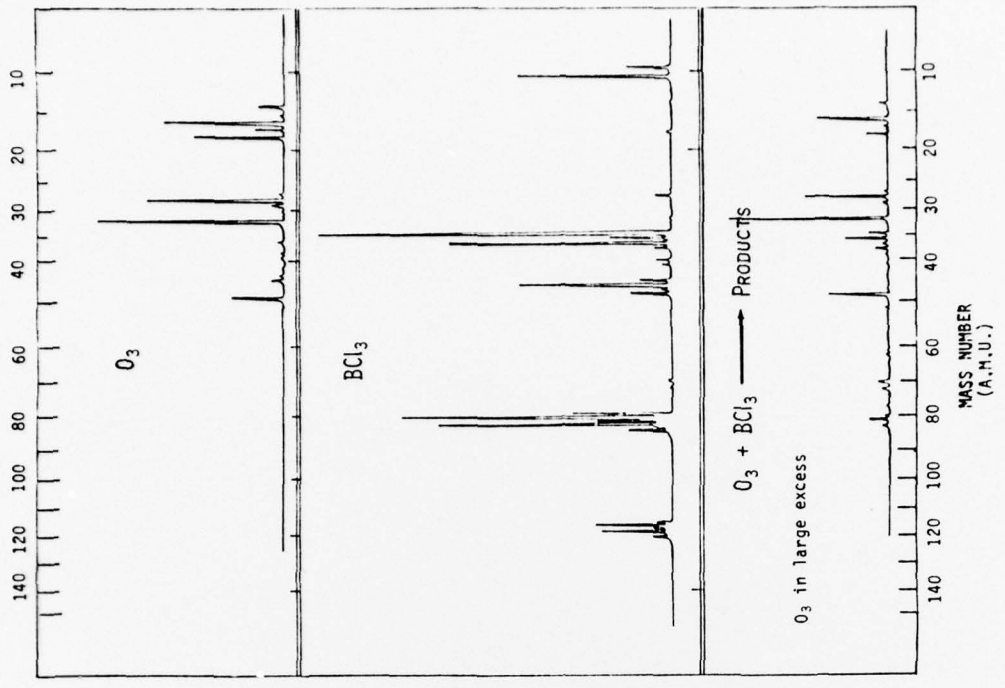
O$_3$+BCl$_3$ ⟶ products

[BCl$_3$]

Time in Minutes

Figure 9a

STOP-FLOW T.O.F. MASS SPECTROMETRY

19

time after mixing a small concentration of BCl_3 with a large excess of ozone. Close examination reveals that the observed product patterns differ substantially from the superposition of the pure O_3 and pure BCl_3 traces. In Table III we have listed those significant mass peaks observed in the mixed O_3/BCl_3 system which were found to be of only minor importance in either pure spectrum. Species such as BO, BO_2, $BClO$, Cl_2 and HCl have been identified. Other significant mass peaks remain unassigned at this time.

Finally, an end product analysis investigation of Reaction (8) was undertaken. Ozone and BCl_3 were mixed in a reaction vessel and allowed to react to completion. The techniques of infrared and uv absorption spectroscopy and expansion of condensable and non-condensable gases into calibrated volumes were utilized in the product analysis. As can be seen in Table IV, the loss of BCl_3 molecules was found to be about 2/3 that of the gain in Cl_2 molecules: chlorine balance seems assured through the formation of Cl_2. Since the number of condensable boron oxide molecules formed could not be measured, the boron and oxygen balances cannot be definitively assigned. One notices, however, that the loss of ozone molecules exceeds the loss of BCl_3 molecules, possibly by as much as a 3:2 ratio. If such stoichiometry is assumed, then the overall Reaction (8) mechanism could be represented by reaction expressions of the type (or linear combinations thereof) listed at the bottom of Table IV.

An abbreviated stop-flow time-of-flight mass spectrometry study was also performed on Reaction (9). This reaction was found to be fast, probably heterogeneous, and produced HCl and condensable boron oxides in high yield. Indeed, the addition of pure BCl_3 to a reaction vessel which had previously contained H_2O resulted in both the fast decay of BCl_3 and the
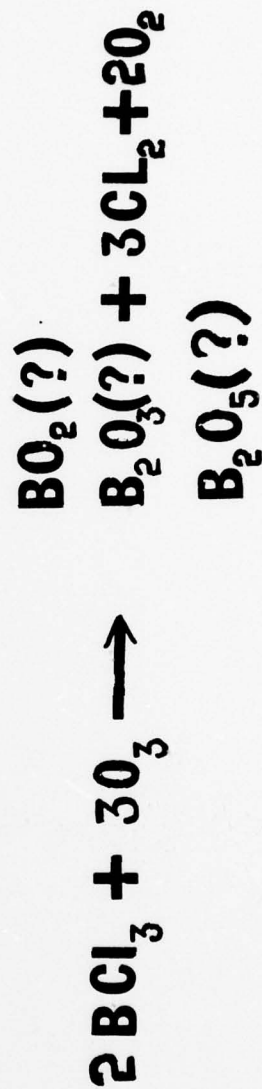
20

TABLE III

SIGNIFICANT MASS SPECTRAL PEAKS OBSERVED IN THE O_3 + BCl_3 SYSTEM WHICH WERE FOUND TO BE OF ONLY MINOR IMPORTANCE IN THE MASS SPECTRA OF PURE O_3 AND/OR PURE BCl_3.

MASS NUMBER	POSSIBLE ASSIGNMENT
26	BO
27	BO
29	?
31	?
34	?
36	HCl
38	HCl
42	BO_2
43	BO_2
51 or 52	?
57	?
62	BClO
63	BClO
64	BClO
70	Cl_2
72	Cl_2
77	?
110	?

TABLE IV

END PRODUCT ANALYSIS

	RUN 1	RUN 2	RUN 3
$-BCL_3$	?	1.3×10^{19} MOLECULES	1.7×10^{19} MOLECULES
$-O_3$	2.3×10^{19} MOLECULES	1.8×10^{19} MOLECULES	2.0×10^{19} MOLECULES
$+CL_2$	2.8×10^{19} MOLECULES	1.9×10^{19} MOLECULES	2.2×10^{19} MOLECULES
$+O_2$	1.5×10^{19} MOLECULES	1.3×10^{19} MOLECULES	1.3×10^{19} MOLECULES

$$BO_2(?)$$
$$2\,BCl_3 + 3O_3 \longrightarrow B_2O_3(?) + 3CL_2 + 2O_2$$
$$B_2O_5(?)$$

obvious formation of HCl. In experiments in which BCl_3 and H_2O were mixed in the gas phase, the molecular leak of the reaction vessel very quickly became clogged resulting in the termination of gas flow into the mass spectrometer analyzer.

The above described studies of Reactions (5) through (9) have resulted in some interesting information concerning the general oxidative behavior of the haloboranes. Equally important, they have provided sufficient knowledge to make possible studies of more plume-relevant processes such as the radical-molecule reaction

$$O(^3P) + BF_3 \longrightarrow \text{Products} . \tag{10}$$

Absolute rate constant measurements for Reaction (10) will be undertaken in the second year of this program. The high concentrations of the $O(^3P)$ species found both in plumes and in the upper atmosphere render this reaction of probable importance to infrared signature interpretation. Furthermore, as a step toward technology development, Reaction (10) may provide valuable information on future kinetic methods for studying reactions involving species such as BF_2, BF, BO, BO_2, BOF, etc. Reactions such as those listed in the November 15, 1977 Grumman Aerospace Corporation Compilation (Contract #F04611-77-C-0054) cannot be kinetically defined until clean methods of producing the subject reactant molecular species are found.

23

FOOTNOTES AND REFERENCES

1. Replacement of the flowing nitrogen spark discharge flashlamp by a closed xenon flashlamp is under consideration. During the hydroxyl radical reaction experiments, a period of time elapsed within which photon signals due entirely to flashlamp firing were detected over time intervals of 30 msec or more. These observations were made with the resonance lamp off and the vacuum housing empty and sealed. Since 30 msec is often long enough to follow several 1/e reactant decay periods, we had little success running experiments with these interfering conditions. Initially we postulated three possible explanations: (1) the flash duration had become greatly extended over its typical ∿20 µsec value; (2) contamination in the flashlamp line was causing an 'afterglow fluorescence' to be emitted from the flashlamp; and (3) flashlamp radiation was inducing long-lived fluorescence emission from the vacuum housing walls, interference filter, etc. None of these explanations proved to be correct. Indeed, the more we cleaned our components the worse the problem became. Eventually, in analogy with superradiant phenomena in nitrogen gas lasers, we realized that our nitrogen stream was so pure that we were observing 'active nitrogen' fluorescence over the 30 msec interval following the 20 µsec flashlamp firing duration. [This emission is inconveniently located near 310-320 nm, explaining its passage through our bandpass filter.] Addition of small traces of oxygen to the spark discharge gas stream allows the afterglow duration to be reduced to 3-5 msec. Unfortunately, oxygen addition also quenches the vacuum ultraviolet emission intensity from the flashlamp, thereby decreasing overall signal levels. Furthermore, because of this 3-5 msec 'afterglow', it is sometimes necessary to reject data from the first few milliseconds following the photolysis flash. Since for large values of k_{exp} (increasingly prevalent as k_{bi} increases at higher temperatures) this time interval corresponds to a good fraction of one 1/e reactant decay period, considerable extra signal averaging becomes necessary upon such data rejection. Use of a xenon flashlamp should eliminate this problem entirely.

2. R. Zellner and W. Steinert, Int. J. Chem. Kinet. **8**, 397-409 (1976).

3. D.L. Baulch and D.D. Drysdale, Evaluated High-Temperature Chemical Kinetic Data, Butterworths, 1977.